The Flinders University of South Australia

OPTICAL MODEL FOR ELECTRON SCATTERING FROM INERT GASES

I.E. McCARTHY, C.J. NOBLE, B.A. PHILLIPS and A.D. TURNBULL

FIAS-R-4

APRIL 1976

OPTICAL MODEL FOR ELECTRON SCATTERING FROM INERT GASES*

I.E. McCarthy, C.J. Noble, B.A. Phillips and A.D. Turnbull

Institute for Atomic Studies

The Flinders University of South Australia
Bedford Park, S.A. 5042, Australia

ABSTRACT

A local, complex potential is used to compute differential cross sections, spin polarizations and total nonelastic cross sections for electrons incident on inert gases at energies ranging from 20eV to 3000eV. Excellent comparison with experimental data is achieved in most cases. In addition to Hartree-Fock wave functions, the input to the model involves two parameters. The strength W of the imaginary potential is determined by fitting the total nonelastic cross section. The static polarizability α is well known from independent determinations.

1. INTRODUCTION.

The optical model for electron scattering from atomic systems has wide application, not only as a description of elastic scattering differential cross sections and spin polarizations and of the total non-elastic cross section, all three of which it describes directly, but also as an essential ingredient of the description of reactions used as probes for atomic and molecular structure, the most successful of which is (e,2e) spectroscopy[1]. In fact another reaction which has been widely used for some years to obtain a limited amount of structure information, (γ,e) or the photoelectric effect[2], owes its most severe limitations to an inadequate description of the final state, for which an optical model should give a good approximation.

The optical model for the electron-atom system is most easily understood in terms of the multichannel expansion. Channels, including ionized channels, are expressed in terms of a discrete notation using indices μ, ν. Box normalization may be used to make the continuum discrete for formal purposes.

The wave function $\Psi^{(+)}(x,\xi)$ for the entire scattering problem is written in terms of target states $\psi_\mu(\xi)$ as

$$\Psi^{(+)}(x,\xi) = \Sigma_\mu \phi_\mu^{(+)}(x)\psi_\mu(\xi). \qquad (1)$$

The coordinate x includes the position $\vec{r}$ and spin $\vec{\sigma}$ coordinates. The superscript (+) indicates outgoing spherical-wave boundary conditions.

The Schrödinger equation for the problem is written in terms of a set of coupled equations

$$[E-\epsilon_\mu-K-V_{\mu\mu}]\phi_\mu^{(+)} = \Sigma_{\mu\neq\nu}V_{\mu\nu}\phi_\nu^{(+)}. \qquad (2)$$

where the interactions $V_{\mu\nu}$ include nonlocal terms enabling antisymmetry for identical fermions to be implicitly included.

The optical model is obtained by formally solving the set (2) for the entrance channel function $\phi_0^{(+)}$.

$$[E-K-V_{00}-V_{0\nu}(E-\epsilon_\mu-K-V_{\mu\nu})^{-1}V_{\mu 0}]\phi_0^{(+)} = 0. \qquad (3)$$

The optical model potential $\tilde{V}$ is divided into two parts

$$\tilde{V} = V_{00}+V_{0\nu}(E-\epsilon_\mu-K-V_{\mu\nu})^{-1}V_{\mu 0}. \qquad (4)$$

The first part is the static interaction V_{00}, which is real and represents the average for the ground state of the potential felt by the incident electron. The second part is complex. Its real part describes virtual excitation of non-elastic channels μ and ν, generally called polarization. The imaginary part represents real excitations of non-elastic channels, often called absorption of electrons from the entrance channel.

In practice approximations must be made to obtain computable equations. The independent-particle approximation is always made. In this approximation $\psi_\mu(\xi)$ is a Slater determinant and the nonlocal part of V_{00} is a set of exchange terms. Some optical models[3,4] make the second order approximation, to the multiple scattering series for the optical model potential $\tilde{V}$ obtained by expanding equation (4). The second order terms are evaluated in the closure approximation by taking an average excitation energy which is selected to ensure the correct asymptotic behaviour for the polarization potential.

The optical model of Furness and McCarthy[5] takes a semiphenomenological approach, evaluating V_{00} by using the screening potential obtained from a Hartree-Fock calculation of the target and an equivalent local approximation to the exchange term, which has been shown by Bransden *et al*[6] and by Riley and Truhlar[7] to give approximately two-figure accuracy in phase shifts at all energies down to a few tenths of a volt, when compared with exact numerical evaluation of the integro-differential equation for scattering from the nonlocal ground state potential V_{00}. The polarization term is the static cut-off polarization term with the static polarizability as a parameter. The absorption term is proportional to the probability $|u_i|^2$ of finding an electron in the single-particle state i and to the energy factor in the local Rutherford scattering cross section at the point r, $[E-V(r)]^{-2}$, where V(r) is the equivalent local potential. The parameter W describing the strength of the absorptive term is obtained by requiring that the total non-elastic cross section be correctly reproduced by the model. The model is nonrelativistic.

2. THE MODEL.

The present work generalizes and improves the model of Furness and McCarthy[5], computing the screening and exchange terms in V_{00} directly from Hartree-Fock orbitals, including relativistic terms, the most important of which is spin-orbit coupling, and correcting a numerical error of a factor of two in the equivalent local exchange potential for closed-shell targets.

The equivalent local relativistic ground state potential for the partial wave ℓ is

$$U_\ell(\rho) = \frac{2(E+mc^2)}{\hbar^2c^2k^2}V - \frac{1}{\hbar^2c^2k^2}V^2 - \frac{1}{\rho}\frac{1}{E-V+2mc^2}\frac{dV}{d\rho}\vec{\sigma}\cdot\vec{\ell}$$

$$+ \frac{1}{2(E-V+2mc^2)}\frac{d^2V}{d\rho^2} + \frac{3}{4}\frac{1}{(E-V+2mc^2)^2}\left(\frac{dV}{d\rho}\right)^2 , \qquad (5)$$

where E is the kinetic energy of the electron in the center-of-mass system, k is the corresponding wave number,

$$\rho = kr \qquad (6)$$

$$V = V_S + V_E. \qquad (7)$$

The screening term $V_S(r)$ is evaluated from tables[8] of the radial Hartree-Fock orbitals $u_i(r)$ as follows.

$$V_S(r) = -e^2\Sigma_i 2(2\ell+1)\int_r^\infty dr' \left(\frac{1}{r} - \frac{1}{r'}\right)u_i(r')^2. \qquad (8)$$

The orbitals are evaluated without including spin-orbit coupling, so that the orbital index i includes only the quantum numbers n and ℓ.

By differentiating equation (8) we obtain the following expressions for the derivatives of V_S.

$$\frac{dV_S}{dr} = e^2\Sigma_i 2(2\ell+1)\frac{1}{r^2}\int_r^\infty dr' u_i(r') , \qquad (9)$$

$$\frac{d^2V_S}{dr^2} = -\frac{2e^2}{r^3}\Sigma_i 2(2\ell+1)\int_r^\infty dr' u_i(r')^2 - e^2\Sigma_i 2(2\ell+1)\frac{1}{r^2}u_i(r)^2. \qquad (10)$$

The equivalent local exchange potential of Furness and McCarthy[5], which is derived from the nonlocal exchange potential by the approximation of Perey and Buck[9] and a local WKB approximation, is for the case of a closed shell target

$$V_E = \frac{1}{2}\left[E-V_S-\{(E-V_S)^2+\alpha^2\}^{\frac{1}{2}}\right],$$

$$\alpha^2 = \frac{4\pi e^2\hbar^2}{mr^2}\Sigma_i u_i(r)^2. \qquad (11)$$

Bransden, McDowell, Noble and Scott[6] have shown that the equivalent local exchange potential (11), provides a reliable approximation to the nonlocal exchange terms even when other potentials, in particular polarization potentials, are included in the calculation. A convenient energy-independent polarization potential is the adiabatic Temkin-Lamkin polarization potential. This is derived from the polarized orbital approximation and has been shown by Temkin and Lamkin[10] to describe dipole distortion effects accurately. Neglecting exchange polarization terms,

$$V_p(r) = -\beta(Zr/a_0)/(Zr/a_0)^4, \qquad (12)$$

where

$$Z^4 = (9a_0^3/2\alpha) \qquad (13)$$

and α is the static polarizability in units of the Bohr radius a_0. The polynomial $\beta(x)$ is

$$\beta(x) = \frac{9}{2} - \frac{2}{3}e^{-2x}\left[x^5+\frac{9}{2}x^4+9x^3+\frac{27}{2}x^2+\frac{27}{2}x+\frac{27}{4}\right]. \qquad (14)$$

This form is used in the present model.

The imaginary optical model potential of Furness and McCarthy, with units chosen so that W is a constant is,

$$W(r) = W\frac{e^2\hbar^2c^2(2\ell+1)}{[E-V(r)]^2}\frac{1}{a_0^2}\Sigma'_j u_j(r)^2 \qquad (15)$$

where the sum over j extends only over orbitals that contribute significantly to the total ionization cross section. In the present model we limit this sum to one orbital, the one at the Fermi level. It was shown by Furness and McCarthy[11] that the choice of the orbital shape is not critical.

3. TOTAL NONELASTIC CROSS SECTIONS.

The simplest number computed by the optical model is the total nonelastic reaction cross section σ_R for a particular incident kinetic energy E and a particular atom.

A large part of σ_R is the total ionization cross section σ_I. A summary of experimental data on σ_I is given by Kieffer and Dunn[12].

Estimates of the remainder of σ_R due to inelastic scattering to discrete states have been made by Jansen[13].

In the present work the values of Jansen for σ_R are used to determine the parameter W in the imaginary potential. The model is required to reproduce the experimental value of σ_R. This is a one-parameter search, which is a fast and simple numerical procedure.

The values of W are of some interest. For all the rare gases except helium there are eight valence electrons contributing most to the ionization cross section σ_I. Six of these belong to the valence p shell, so the shape of the squared valence p orbital is used in (15). Only a very slight shape modification is effected by adding the squared valence s orbital. If the form factor (15) is a good description of the reaction one would expect all values of W to be the same, independent of the energy or the atom.

Alternatively, using the model (15) one might ask how well the reaction cross section σ_R is predicted as a function of energy for each atom. Fig. 1 shows the values of W that reproduce the correct σ_R. They in fact increase slowly and smoothly with energy. The values for the four p-shell atoms are quite close and helium is rather different. The value of W is of course zero below the first excitation threshold. Its smooth increase with energy confirms the general validity of the optical model.

4. DIFFERENTIAL ELASTIC SCATTERING CROSS SECTIONS.

With the parameter W determined as in section 3 and using the well-known values[14] of the static polarizability α, we have a predictive model for the differential elastic scattering cross section, in which there are no free parameters.

At angles below 50° we have the absolute data of Jansen *et al*[15]. For larger angles there are absolute data due to Williams and Crowe[16] and Williams and Willis[17] and unnormalized data due to Lewis *et al* and Buckman *et al*[18], which are normalized by fitting them to the model and to the data of Jansen *et al*.

Fig. 2 shows the comparison of the model with data between 100eV and 750eV for (a) helium, (b) neon, (c) argon, (d) krypton and (e) xenon.

Fig. 3 shows the comparison for (a) neon, (b) argon, (c) krypton and (d) xenon for energies down to 20eV, where the model still gives an excellent description both of shapes and absolute magnitudes.

Fig. 4 shows that the model accurately describes the scattering for all five gases at (a) 1000eV, (b) 2000eV and (c) 3000eV.

5. SPIN POLARIZATION.

The third entrance channel phenomenon described by the optical model is the spin polarization. For atoms, spin polarization is produced entirely by the Thomas spin-orbit coupling potential.

Experience with the nuclear optical model[19] has shown that the shape of the angular distribution of spin polarization is similar to the derivative of the differential cross section. This is borne out by the calculations of fig. 5 for (a) helium and neon, (b), (c) argon, (d) krypton and (e) xenon.

The spin polarization data are due to Schackert[20]. Dashed curves in some parts of the figure show for comparison the results of a calculation by the method of Bunyan and Schonfelder[21], which uses a real potential given by an effective radially-dependent nuclear charge.

Detailed agreement between theory and experiment is not obtained as it is for the differential cross section, although it is much better for the larger spin polarizations in the case of xenon than for the smaller values with other atoms. This is surprising in view of the excellence of the model in other respects and the simplicity of the spin polarization description.

6. CONCLUSIONS.

The optical model provides an excellent description of entrance channel phenomena from 20eV to 3000eV for electrons incident on inert gas atoms.

One parameter, the imaginary strength W, varies smoothly with energy and makes sense in terms of a physical description of ionization, the main mechanism for absorption of flux from the entrance channel. This parameter is of course not a free parameter for differential cross sections if one regards it as determined by the total nonelastic cross section.

The other parameter of the model, the static polarizability α, provides a good description of small angle scattering where the polarization potential has its greatest effect. Since α has been independently determined, it is not a free parameter.

In view of the general good agreement between experiment and theory, in absolute magnitude of cross sections as well as angular distribution shapes, one must regard it at least as a good interpolation procedure for data. In this light one should perhaps question data where the interpolation appears to break down.

The lack of detailed agreement for spin polarization is a disappointment, although the general agreement for other phenomena, the derivative relationship that exists between differential cross sections and spin polarizations, and the rough agreement with data give the model some credibility in this regard.

The great virtue of the model is its extreme simplicity. Results for closed shell atoms can be computed in a few seconds. This must be contrasted with the optical models of references 3 and 4. In addition to providing a fast and reliable method for calculating entrance-channel phenomena, the model makes possible distorted-wave calculations of more complicated reactions such as inelastic scattering and (e,2e).

REFERENCES AND FOOTNOTES.

*Supported by the Australian Research Grants Committee.

1. I.E. McCarthy and E. Weigold, Physics Reports (to be published).

2. D.A. Shirley (Ed.), Electron Spectroscopy, North-Holland (Amsterdam) 1972.

3. F.W. Byron Jr. and C.J. Joachain, Phys. Letters 49A, 306 (1974) and Phys. Rev. A (to be published).

4. R. Vanderpoorten, J. Phys. B 8, 926 (1975).

5. J.B. Furness and I.E. McCarthy, J. Phys. B 6, 2280 (1973).

6. B.H. Bransden, M.R.C. McDowell, C.J. Noble and T. Scott, J. Phys. B (in press).

7. M.E. Riley and D.G. Truhlar, J. Chem. Phys. 63, 2182 (1975).

8. C. Froese-Fischer, Atomic Data 4, 301 (1972).

9. F.G. Perey and B. Buck, Nucl. Phys. 32, 353 (1962).

10. A. Temkin and J.C. Lamkin, Phys. Rev. 121, 788 (1961); H.S.W. Massey and E.H.S. Burhop, Electronic and ionic impact phenomena, Vol. I, Oxford, 1969, P513.

11. J.B. Furness and I.E. McCarthy, J. Phys. B 6, L42 (1973).

12. L.J. Kieffer and G.H. Dunn, Rev. Mod. Phys. 38, 2 (1966).

13. R.H.J. Jansen, Ph.D. thesis, FOM Institute, Amsterdam (unpublished).

14. Landolt-Bornstein, Zahlenwerte u. Funktionen Vol. I, Springer (Berlin) Part 1, P401.

15. R.H.J. Jansen, F.J. de Heer, H.J. Luyken, B. Van Wingerden and H.J. Blaauw, J. Phys. B 9, 185 (1976); R.H.J. Jansen and F.J. de Heer, *ibid* p.213.

16. J.F. Williams and A. Crowe, J. Phys. B 8, 2233 (1975).

17. J.F. Williams and B.A. Willis, J. Phys. B 8, 1670 (1975).

18. B.R. Lewis, J.B. Furness, P.J.O. Teubner and E. Weigold, J. Phys. B 7, 1083 (1974); B.R. Lewis, I.E. McCarthy, P.J.O. Teubner and E. Weigold, J Phys. B 7, 2549 (1974); S.J. Buckman, P.J.O. Teubner and H. Arriola (to be published).

19. P.E. Hodgson, The optical model of elastic scattering, Clarendon (Oxford), 1963.

20. K. Schackert, Z. Phys. 213, 316 (1968).

21. P.J. Bunyan and J.L. Schonfelder, Proc. Phys. Soc. (London) 85, 455 (1965).

FIGURE CAPTIONS

Fig. 1 The values of the dimensionless imaginary potential strength parameter W, for the indicated targets, which give the experimental[12,13] values of the total nonelastic reaction cross section σ_R.

Fig. 2 Comparison of the present optical model with differential cross section data between 100eV and 750eV for inert gases from helium through xenon. Filled circles describe the data of reference 15, open circles are for references 16 and 17 and crosses are for reference 18.

Fig. 3 Comparison of the present optical model with lower-energy data. Details are given in the caption of fig. 2.

Fig. 4 Comparison of the present optical model with the data of reference 15 for (a) 1000eV, (b) 2000eV and (c) 3000eV for inert gases from helium through xenon.

Fig. 5 Comparison of the present optical model (full curves) with the spin polarization data of reference 20 for inert gases from helium through xenon at the indicated energies. The theory of reference 21 is shown for comparison.

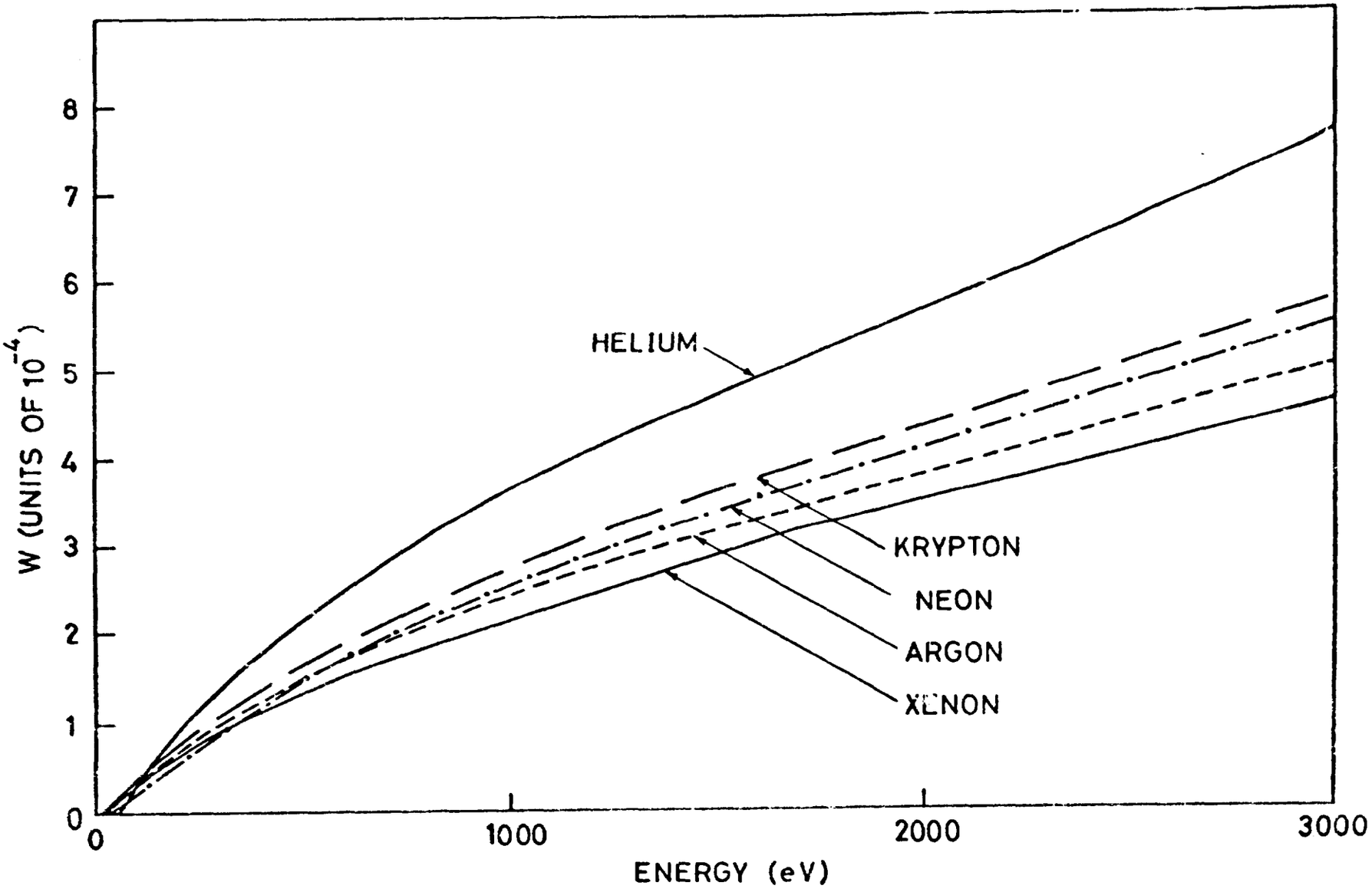
W (UNITS OF 10^{-4})
0
1
2
3
4
5
6
7
8
0
1000
2000
3000
ENERGY (eV)
HELIUM
KRYPTON
NEON
ARGON
XENON

Fig. 1.

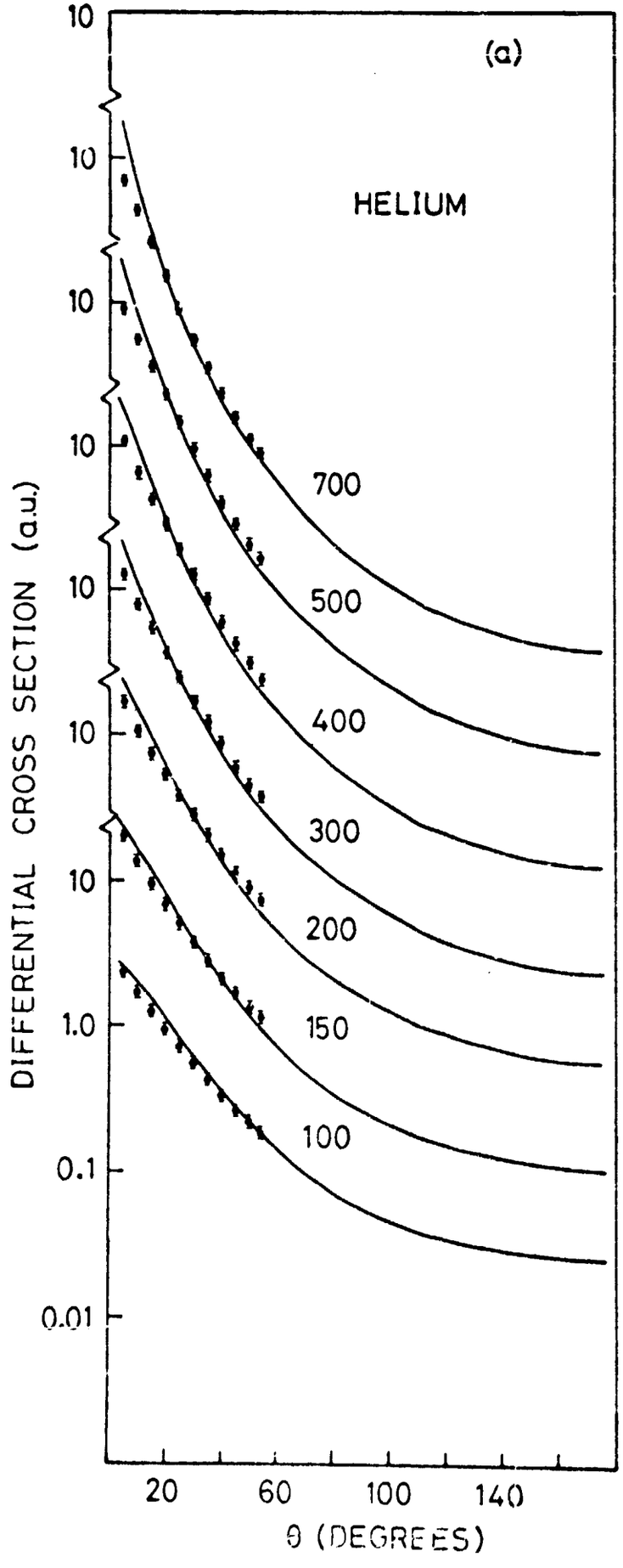
(a)
HELIUM
700
500
400
300
200
150
100
DIFFERENTIAL CROSS SECTION (a.u.)
10
10
10
10
10
10
1.0
0.1
0.01
20
60
100
140
θ (DEGREES)

Fig. 2(a)

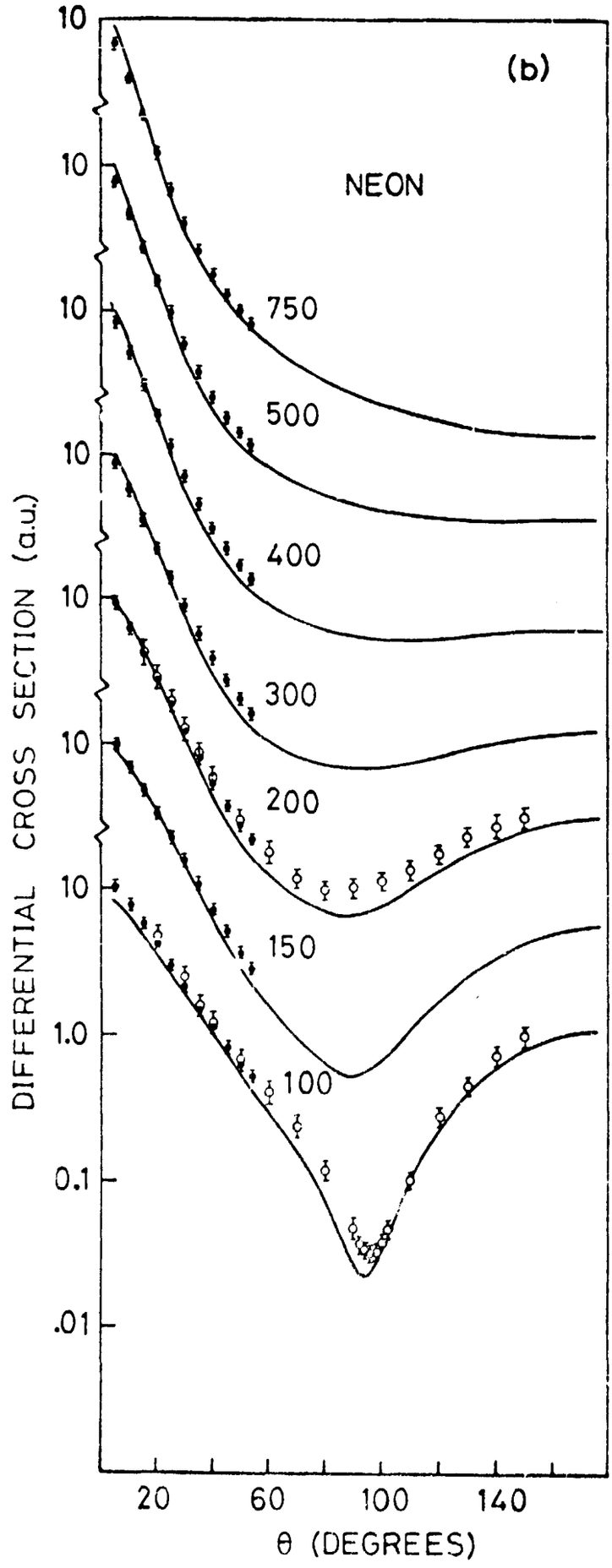
(b)
NEON
750
500
400
300
200
150
100
DIFFERENTIAL CROSS SECTION (a.u.)
10
10
10
10
10
10
1.0
0.1
.01
20
60
100
140
θ (DEGREES)

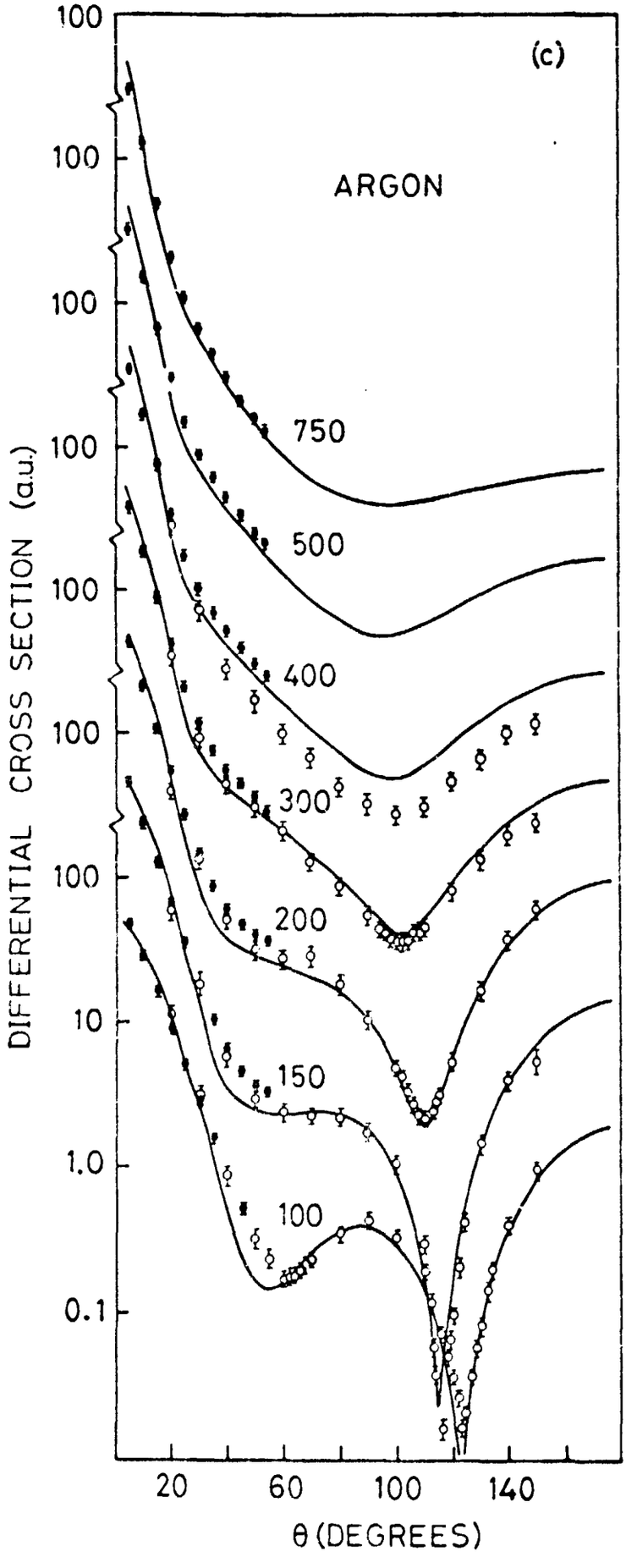
(c)
ARGON
750
500
400
300
200
150
100
DIFFERENTIAL CROSS SECTION (a.u.)
100
100
100
100
100
10
1.0
0.1
20
60
100
140
θ (DEGREES)

Fig. 2(c)

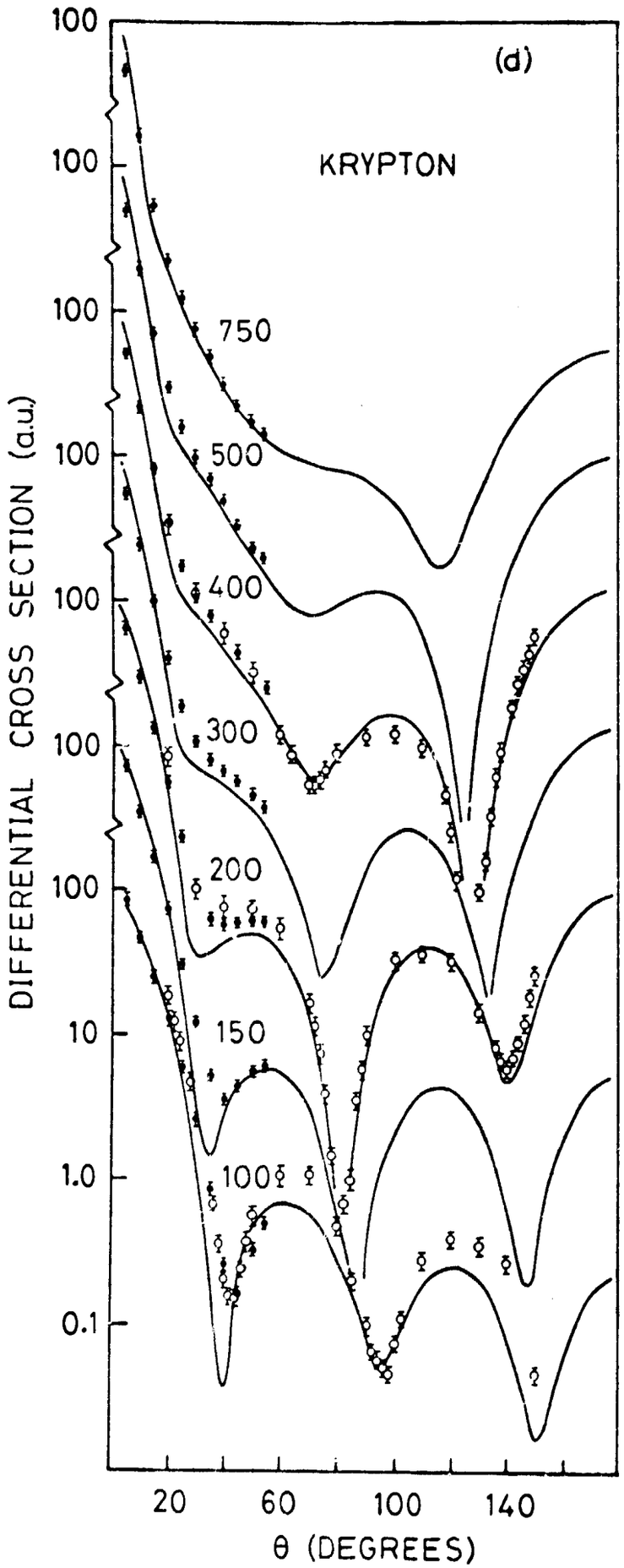
(d)
KRYPTON
750
500
400
300
200
150
100
DIFFERENTIAL CROSS SECTION (a.u.)
100
100
100
100
100
10
1.0
0.1
20
60
100
140
θ (DEGREES)

Fig. 2(d)

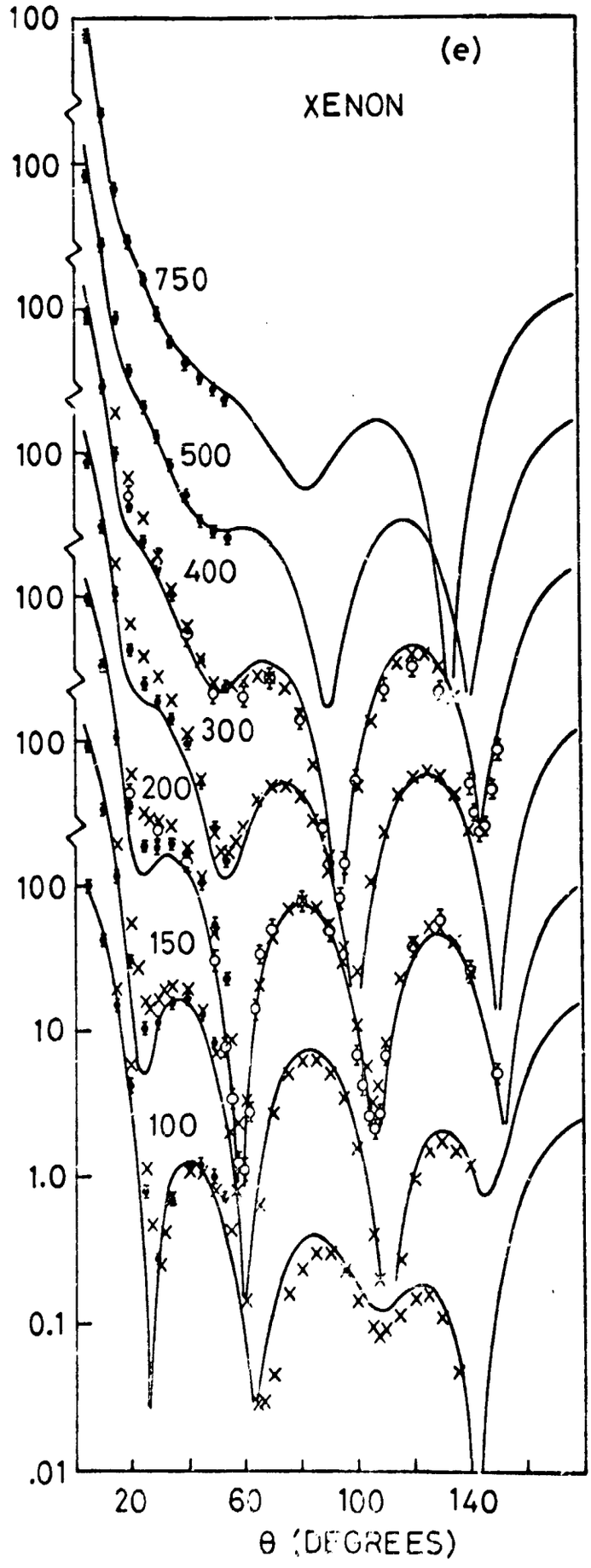
(e)
XENON
750
500
400
300
200
150
100
100
100
100
100
100
10
1.0
0.1
.01
20
60
100
140
θ (DEGREES)

Fig. 2(e)

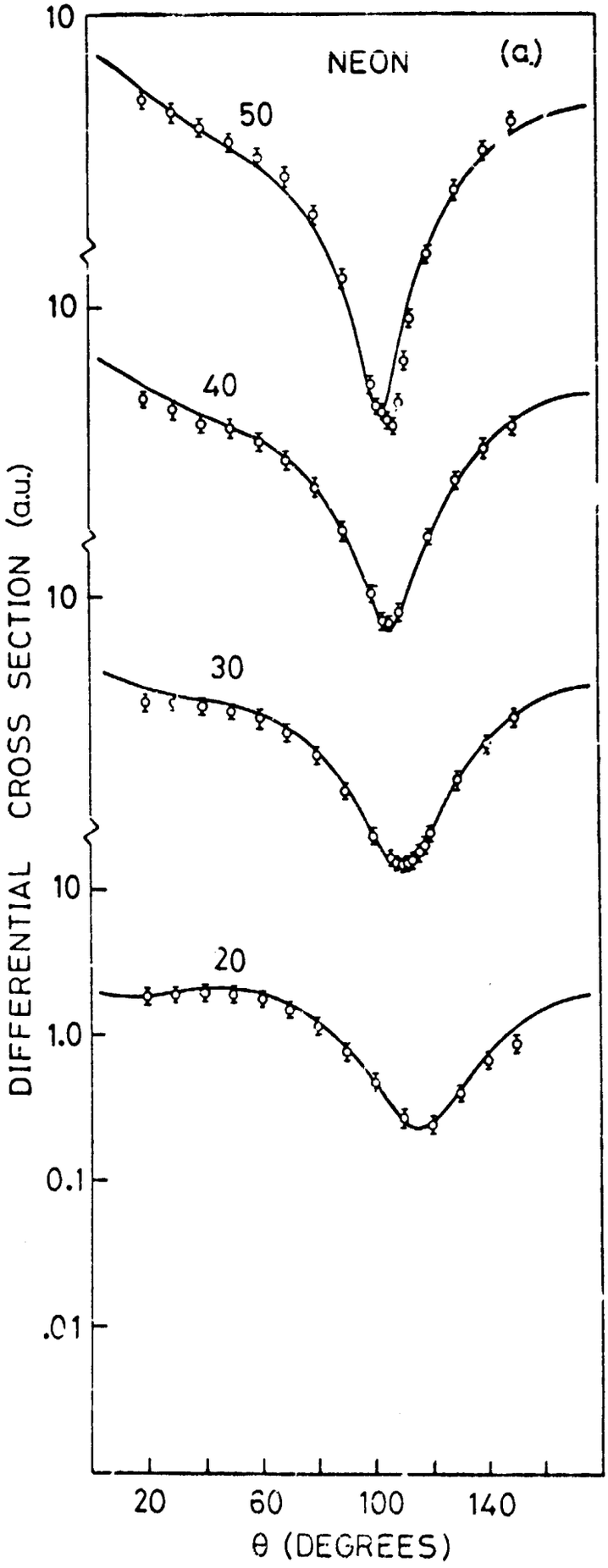
NEON
(a.)
50
40
30
20
10
10
10
10
1.0
0.1
.01
DIFFERENTIAL CROSS SECTION (a.u.)
20
60
100
140
θ (DEGREES)

Fig. 3(a)

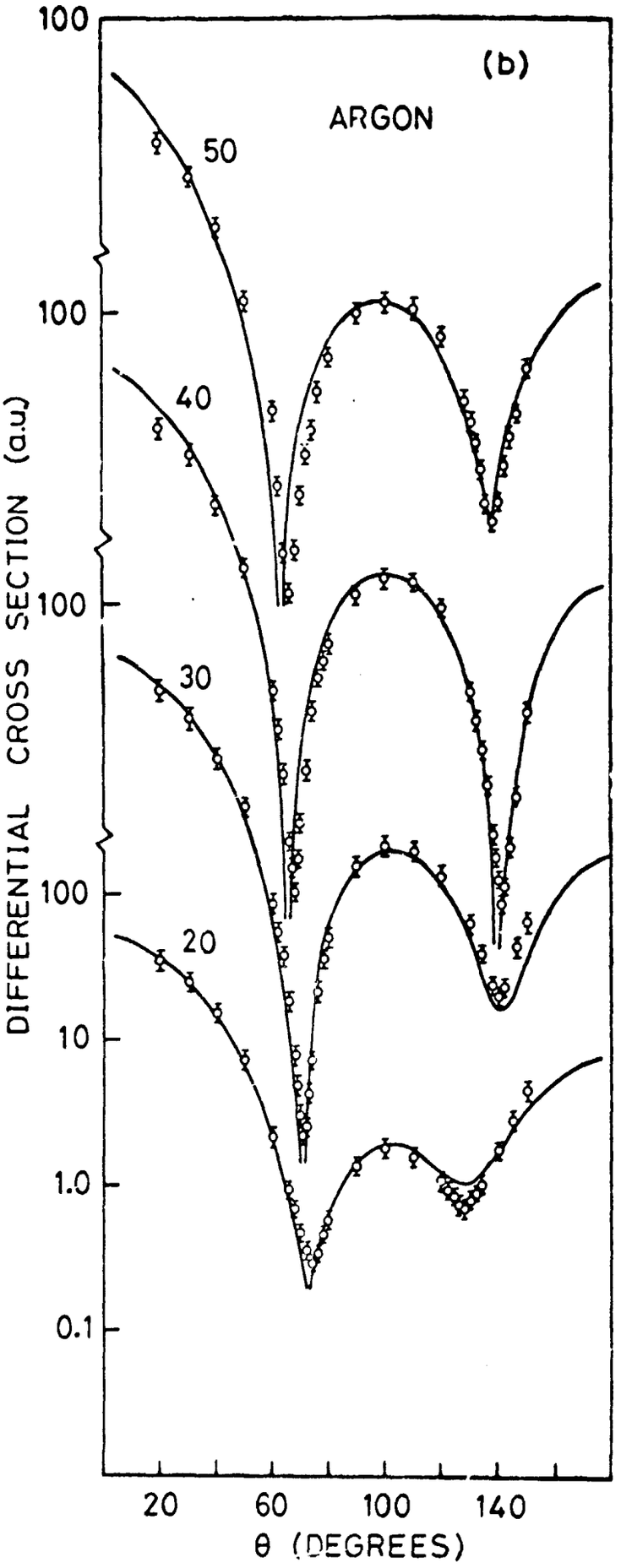
(b)
ARGON
50
40
30
20
100
100
100
100
10
1.0
0.1
DIFFERENTIAL CROSS SECTION (a.u.)
20
60
100
140
θ (DEGREES)

Fig. 3(b)

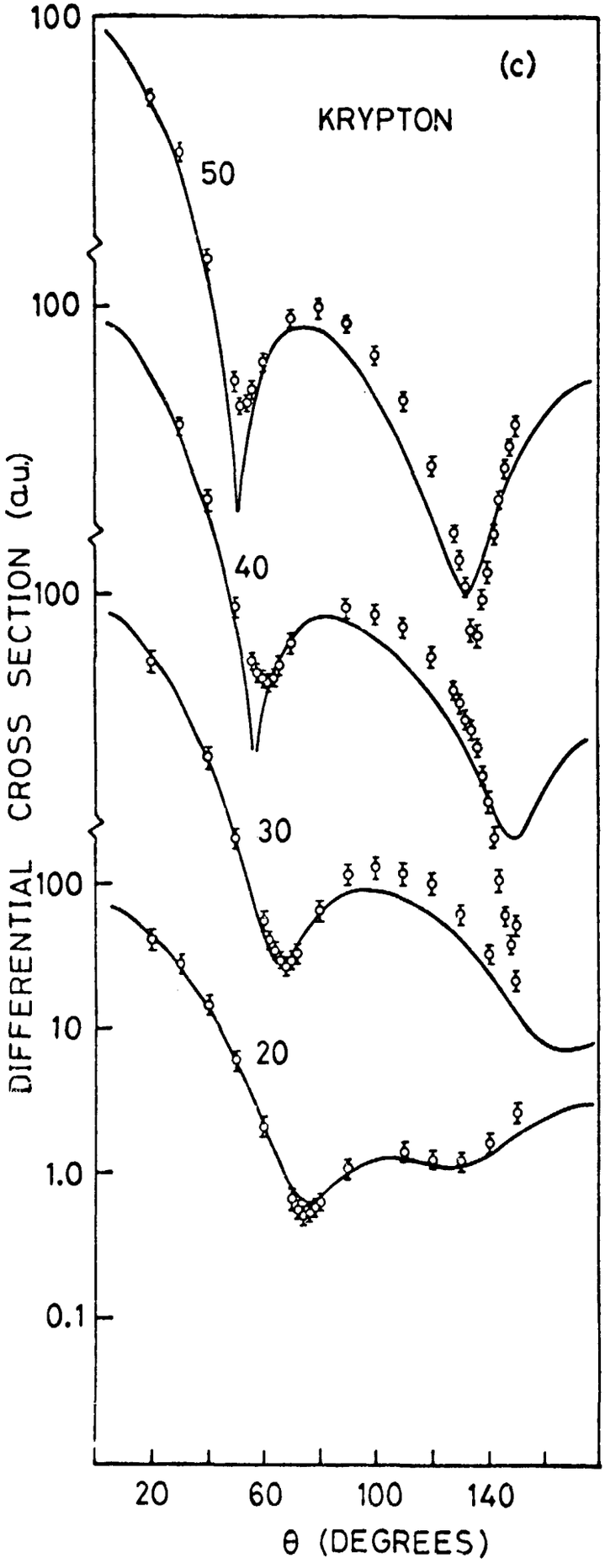
(c)
KRYPTON
50
40
30
20
100
100
100
100
10
1.0
0.1
DIFFERENTIAL CROSS SECTION (a.u.)
20
60
100
140
θ (DEGREES)

Fig. 3(c)

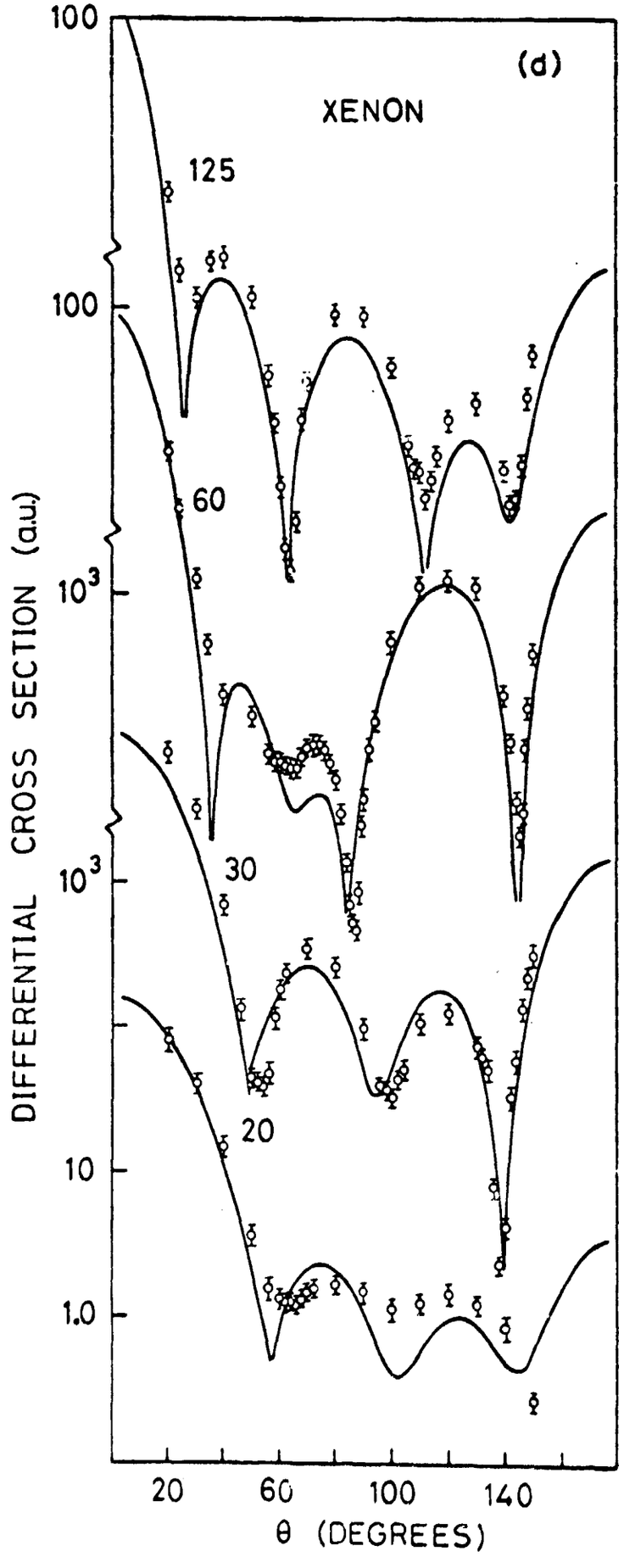
(d)
XENON
125
60
30
20
100
10^3
10^3
10
1.0
DIFFERENTIAL CROSS SECTION (a.u.)
20
60
100
140
θ (DEGREES)

Fig. 3(d)

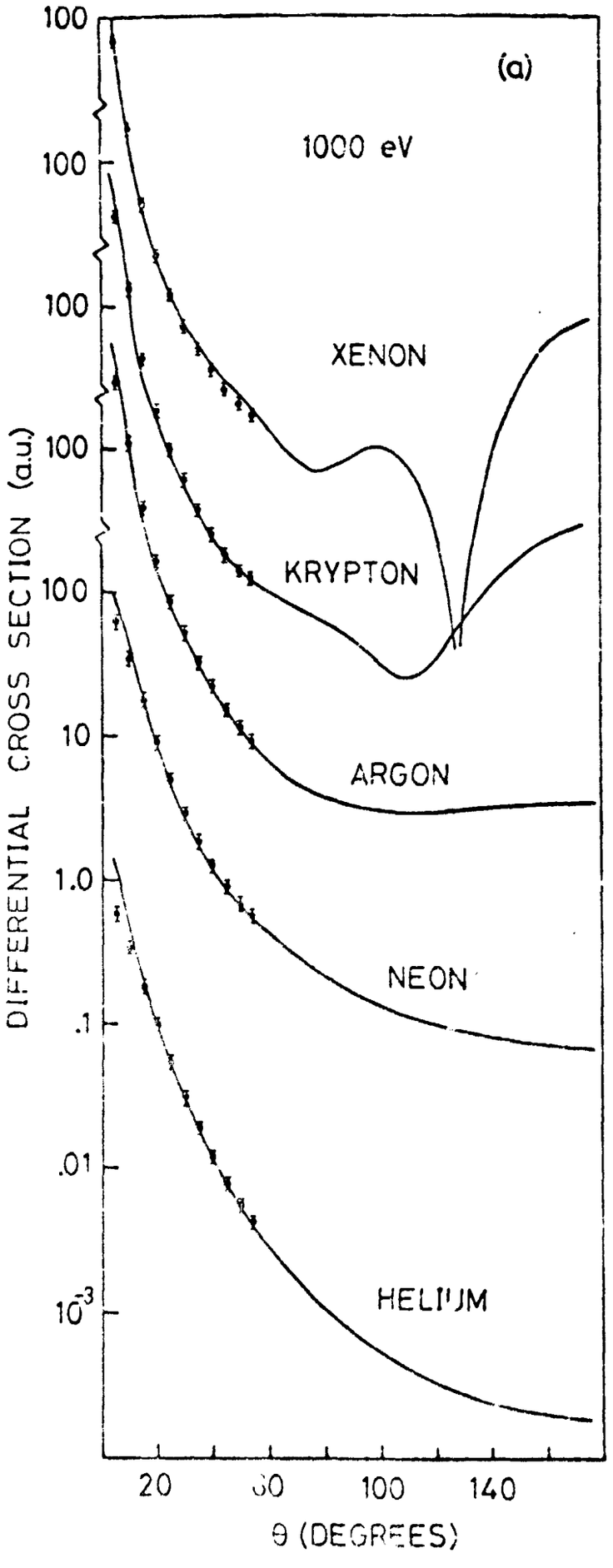
(a)
1000 eV
XENON
KRYPTON
ARGON
NEON
HELIUM
DIFFERENTIAL CROSS SECTION (a.u.)
100
100
100
100
10
1.0
.1
.01
10^{-3}
20
30
100
140
θ (DEGREES)

Fig. 4(a)

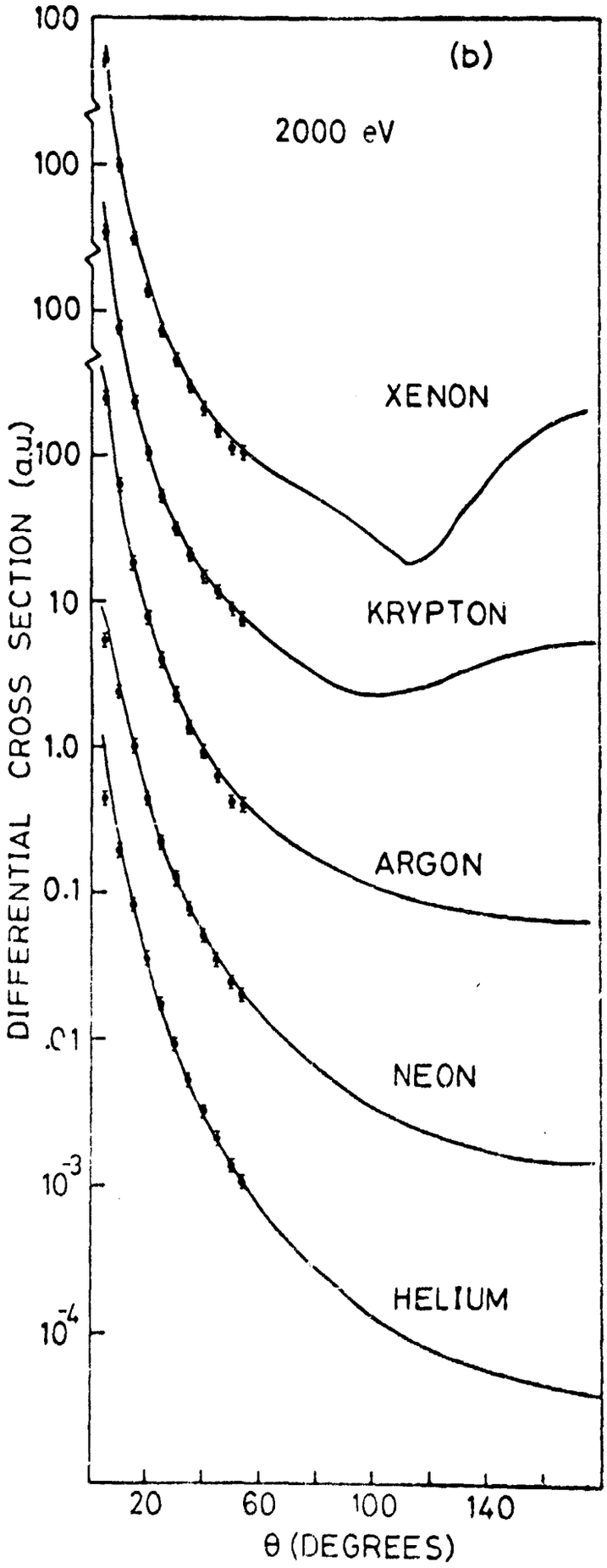
(b)
2000 eV
XENON
KRYPTON
ARGON
NEON
HELIUM
DIFFERENTIAL CROSS SECTION (a.u.)
100
100
100
100
10
1.0
0.1
.01
10^{-3}
10^{-4}
20
60
100
140
θ (DEGREES)

Fig. 4(b)

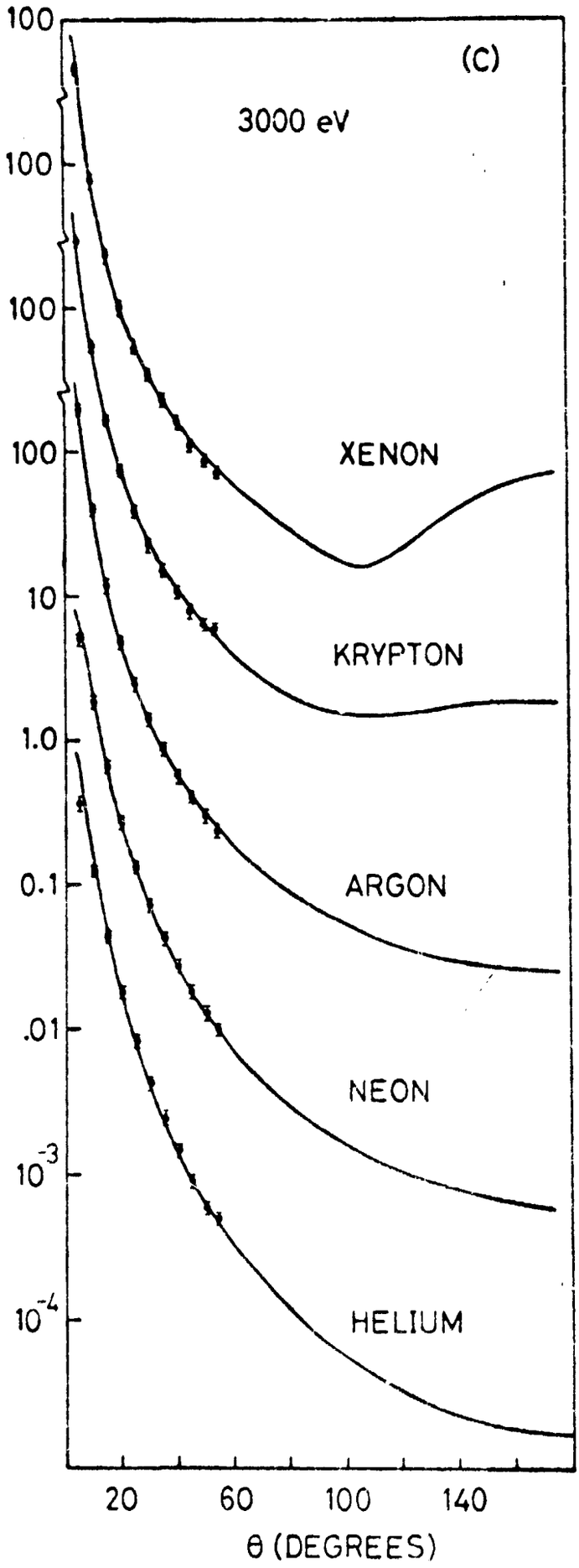
(C)
3000 eV
XENON
KRYPTON
ARGON
NEON
HELIUM
100
100
100
100
10
1.0
0.1
.01
10^{-3}
10^{-4}
20
60
100
140
θ (DEGREES)

Fig. 4(c)

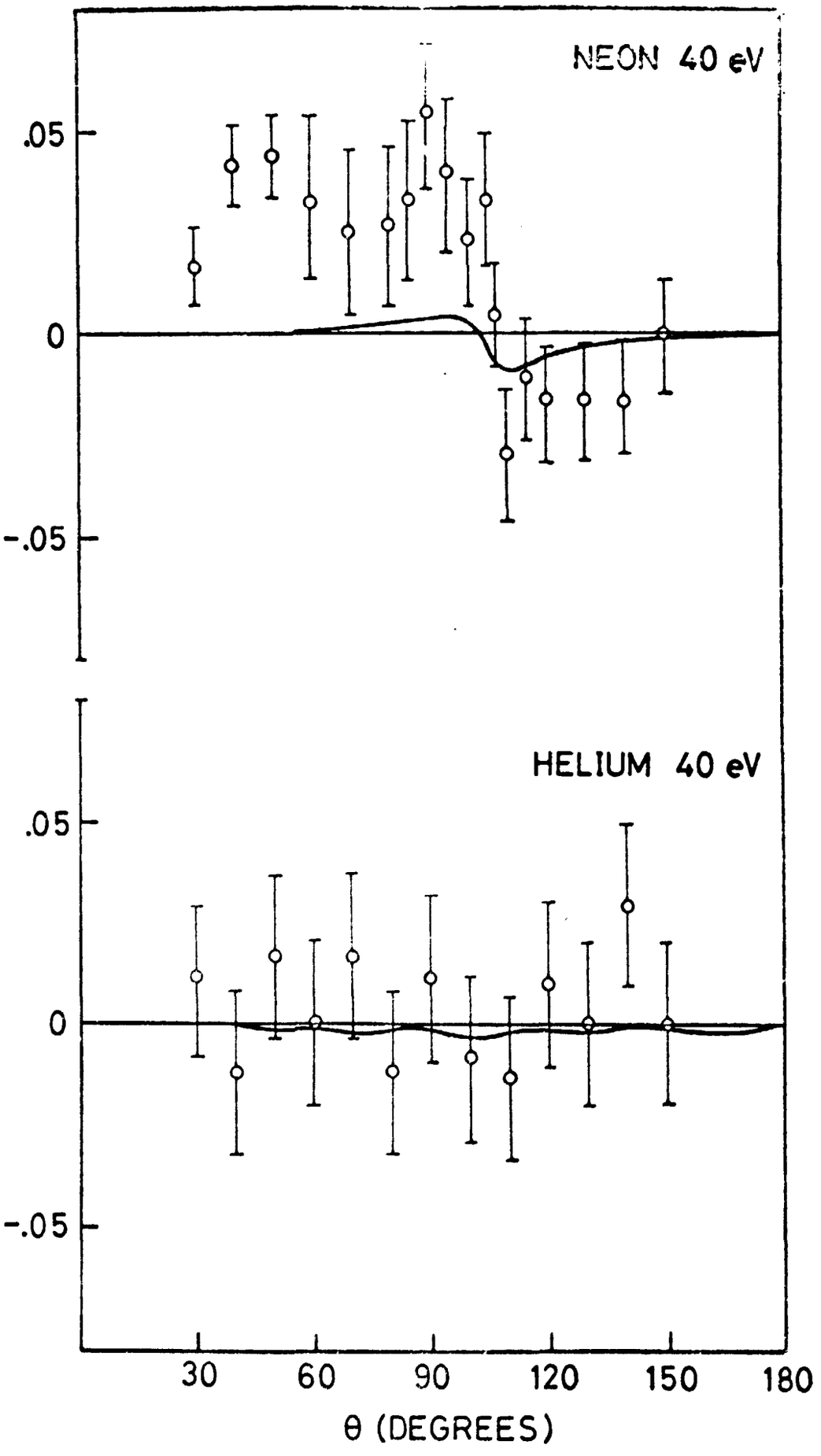
NEON 40 eV
.05
0
-.05
HELIUM 40 eV
.05
0
-.05
30
60
90
120
150
180
θ (DEGREES)

Fig. 5(a)

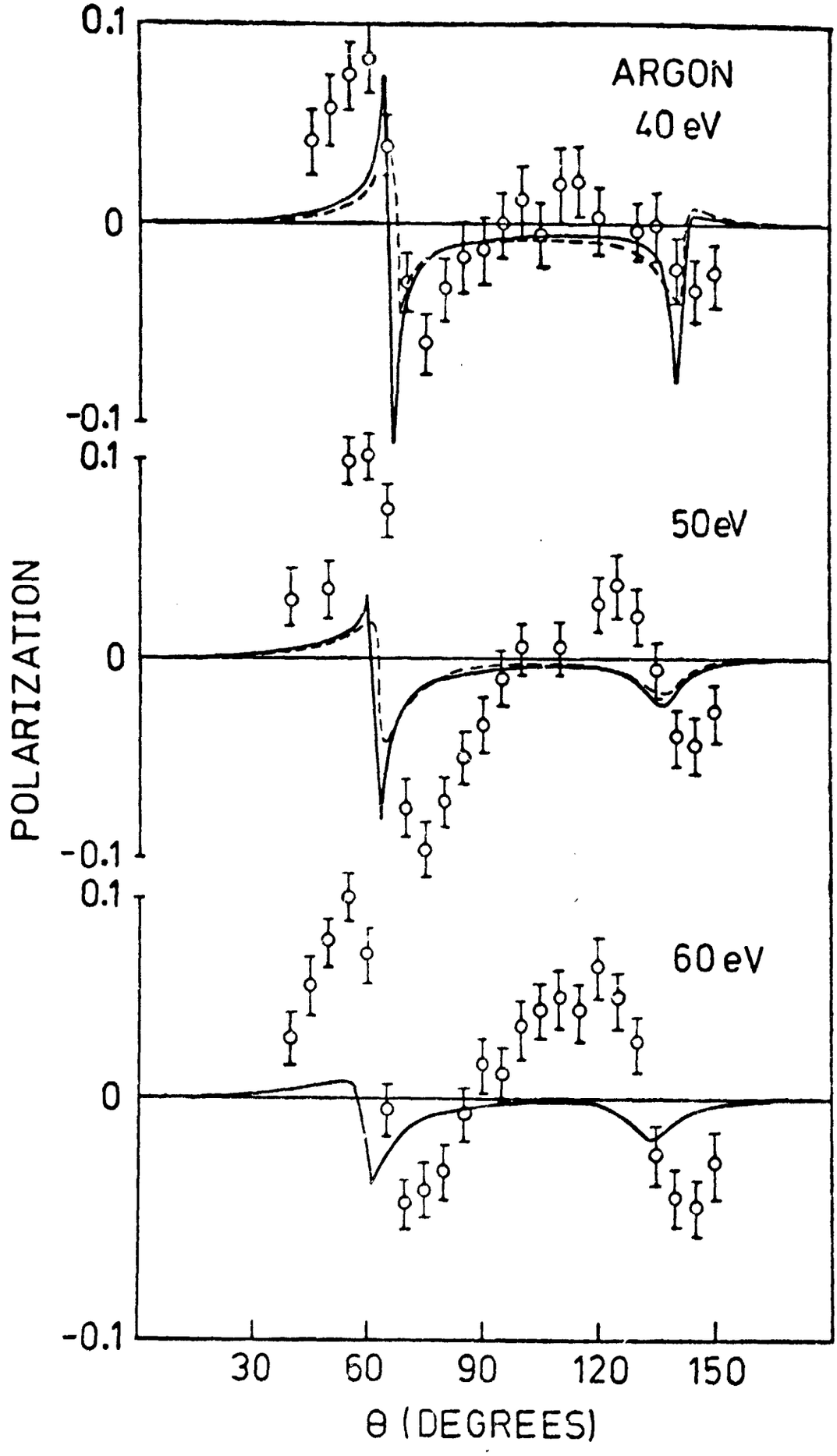
ARGON
40 eV
50eV
60 eV
POLARIZATION
0.1
0
-0.1
30
60
90
120
150
θ (DEGREES)

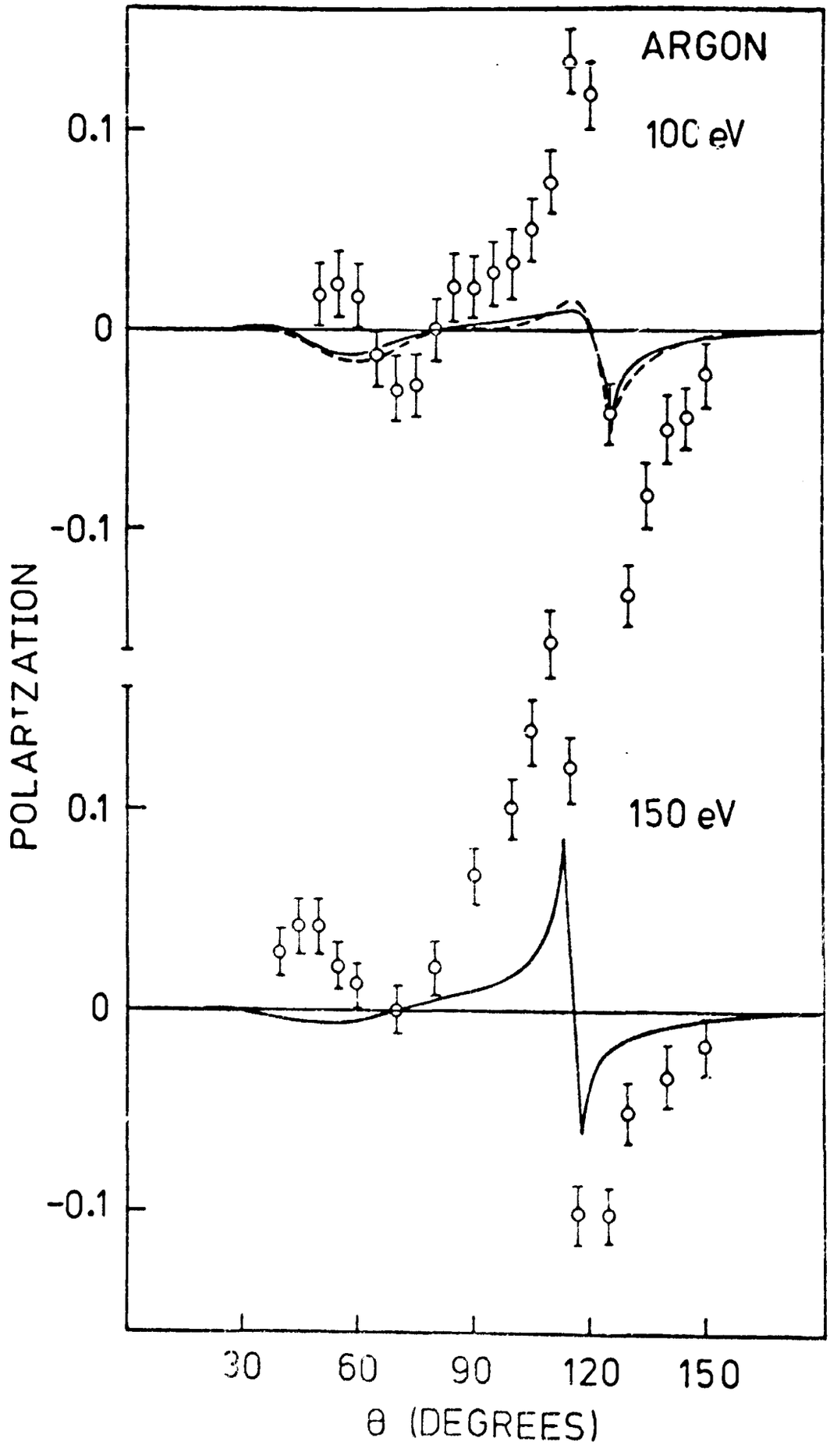
ARGON
100 eV
150 eV
0.1
0
-0.1
0.1
0
-0.1
POLARIZATION
30
60
90
120
150
θ (DEGREES)

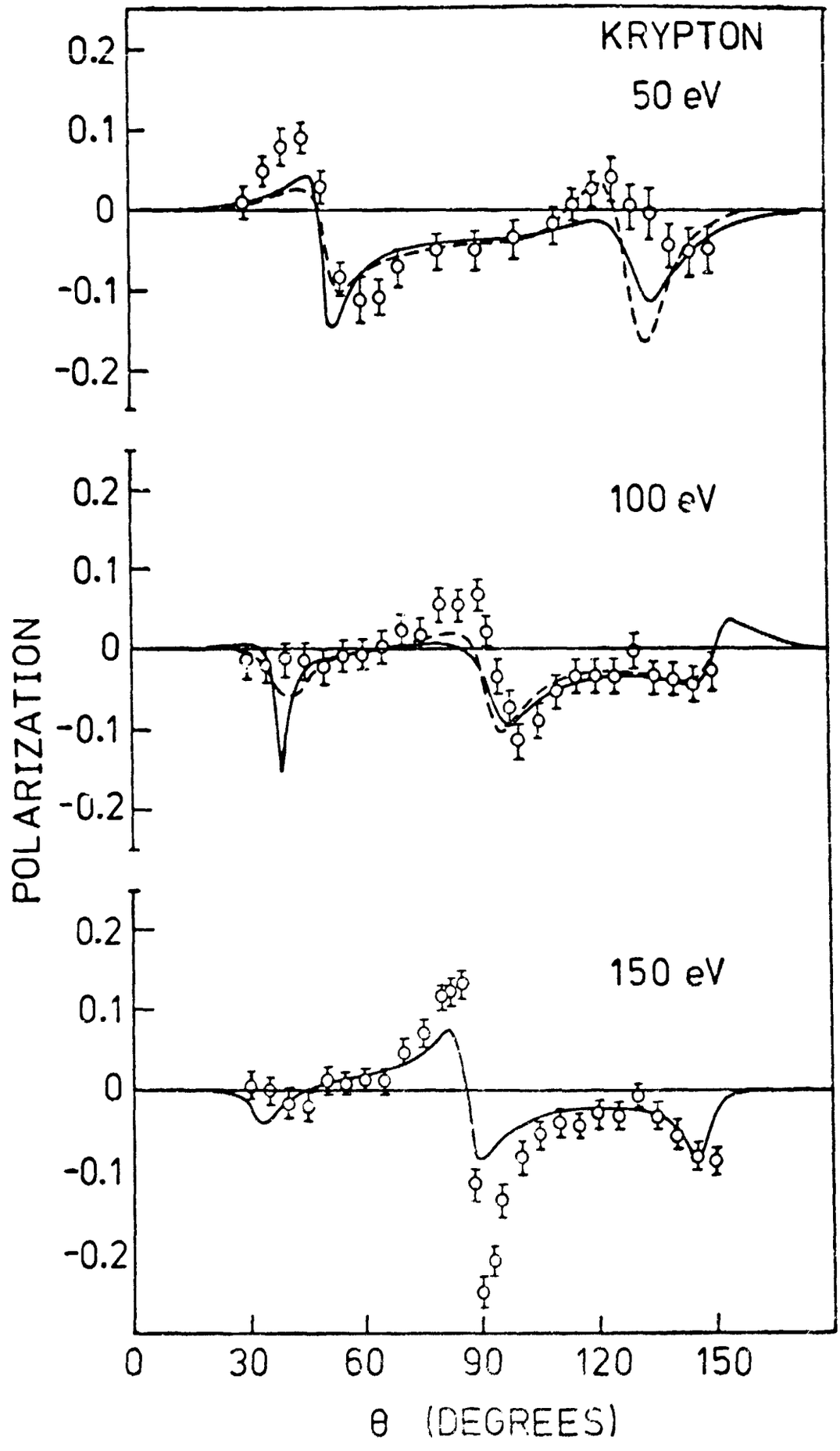
KRYPTON
50 eV
100 eV
150 eV
POLARIZATION
0.2
0.1
0
-0.1
-0.2
0
30
60
90
120
150
θ (DEGREES)

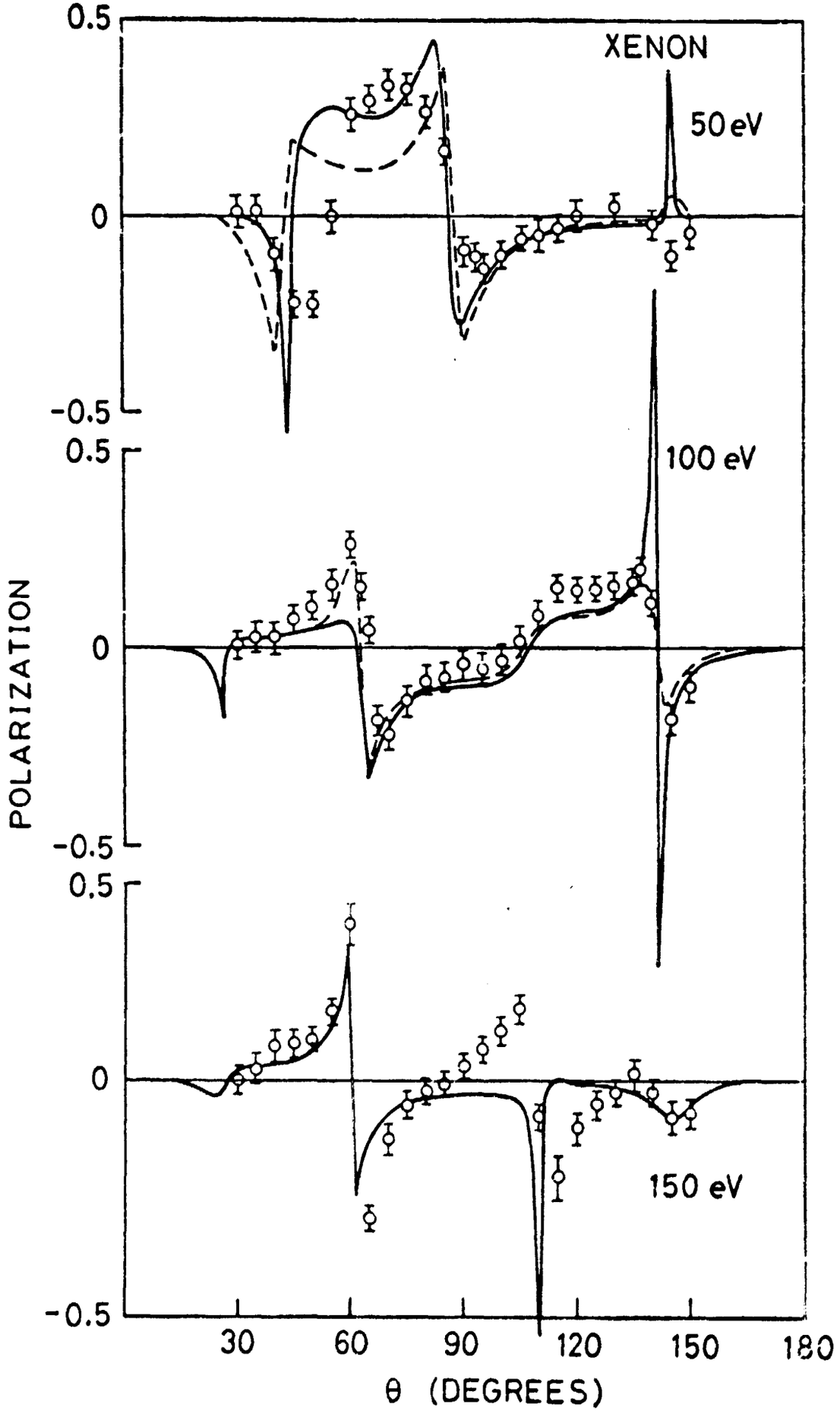
XENON
50 eV
100 eV
150 eV
0.5
0
-0.5
POLARIZATION
30
60
90
120
150
180
θ (DEGREES)

Fig. 5(e)